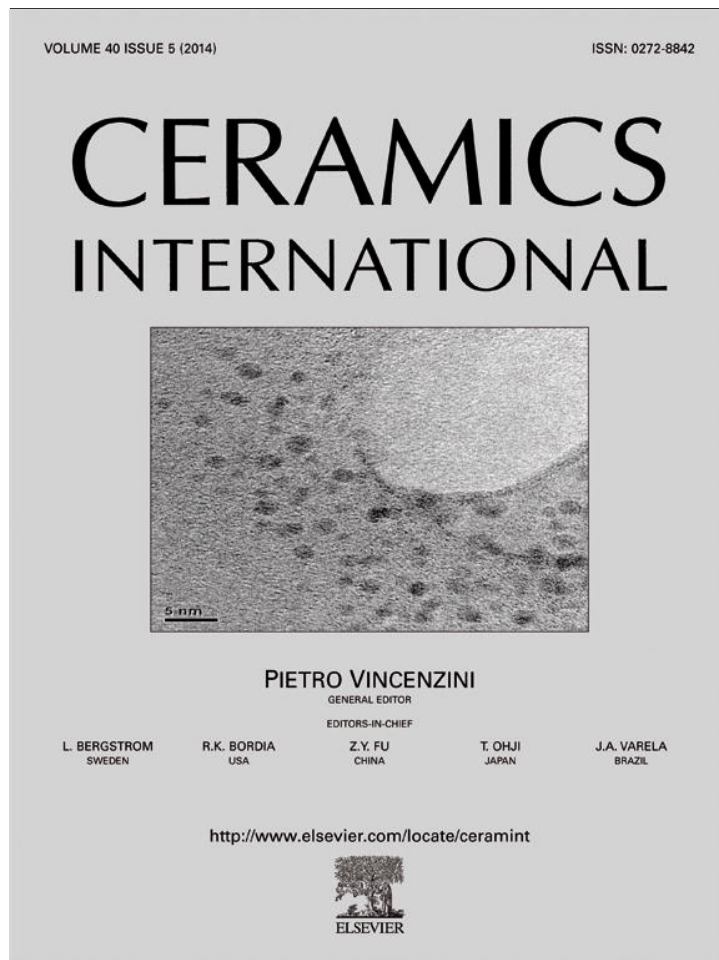


Provided for non-commercial research and education use.  
Not for reproduction, distribution or commercial use.



This article appeared in a journal published by Elsevier. The attached copy is furnished to the author for internal non-commercial research and education use, including for instruction at the authors institution and sharing with colleagues.

Other uses, including reproduction and distribution, or selling or licensing copies, or posting to personal, institutional or third party websites are prohibited.

In most cases authors are permitted to post their version of the article (e.g. in Word or Tex form) to their personal website or institutional repository. Authors requiring further information regarding Elsevier's archiving and manuscript policies are encouraged to visit:

<http://www.elsevier.com/authorsrights>



# Influence of the synthesis process on the features of $Y_2O_3$ -stabilized $ZrO_2$ powders obtained by the sol–gel method

Nadia Mamana<sup>a</sup>, Antonio Díaz-Parralejo<sup>b</sup>, Angel L. Ortiz<sup>b</sup>, Florentino Sánchez-Bajo<sup>c</sup>,  
Ricardo Caruso<sup>a,\*</sup>

<sup>a</sup>Laboratorio de Materiales Cerámicos, Instituto de Física Rosario (CONICET-UNR), Avda. 27 de febrero 210 Bis, 2000 Rosario, Argentina

<sup>b</sup>Departamento de Ingeniería Mecánica, Energética y de los Materiales, Universidad de Extremadura, Avda. de Elvas s/n, 06006 Badajoz, Spain

<sup>c</sup>Departamento de Física Aplicada, Universidad de Extremadura, Avda. de Elvas s/n, 06006 Badajoz, Spain

Received 6 November 2013; accepted 18 November 2013

Available online 3 December 2013

## Abstract

$Y_2O_3$ -stabilized  $ZrO_2$  (YSZ) powders have been prepared by the sol–gel method using different synthesis parameters. Specifically, zirconium *n*-propoxide was dissolved in propanol at pH 0.5 or 5 (provided by  $HNO_3$ ), with or without acetic acid in the hydrolysis medium. Subsequently, the YSZ powders obtained by gelation and drying of these solutions was characterized using scanning and transmission electron microscopies, X-ray diffractometry, and  $N_2$ -adsorption. Compacts made from these YSZ powders which were then sintered were also analyzed. It was found that the pH of the hydrolysis medium has a notable influence on the microstructure, morphology, color, crystallinity, and sintering behavior process of these YSZ sol–gel powders. It was also found that the use of acetic acid also affects the YSZ powder features, and results in compacts with higher residual porosity after sintering. Finally, the compacts prepared from the YSZ powders obtained at pH 5 and without acetic acid exhibit the greatest sinterability.

© 2013 Elsevier Ltd and Techna Group S.r.l. All rights reserved.

**Keywords:** D.  $ZrO_2$ ; Sol–gel; Powder; Synthesis; Densification

## 1. Introduction

In the last decade much attention has been devoted to the development of  $ZrO_2$ -based powders, and in particular to  $ZrO_2$  stabilized by  $Y_2O_3$ . One of these is  $ZrO_2$  with 3 mol%  $Y_2O_3$  properly fabricated so as to have a fine-grained microstructure formed entirely by the tetragonal polymorph (i.e., Y-TZP), which is known to exhibit a very high fracture toughness and also high strength [1,2].

Dry pressing is without any doubt one of the most-extensively used methods for the industrial production of polycrystalline ceramics in general, and of Y-TZP ceramics in particular. It is well known that the quality of the ceramic bodies obtained by dry pressing is strongly influenced by the starting powder, whose characteristics, such as particle sizes, homogeneity, and purity,

condition the sinterability. Note for example that the powders with good compaction behaviors result in higher green-body densifications, and therefore in improved sinterability [3]. Also note that the majority of the defects observed in the sintered ceramics have their origin in the green-body compaction, and are due to powder characteristics. The powder reactivity during sintering is conditioned by the particle sizes and the surface area. However, it is common in powder processing that the primary particles form agglomerates, whose characteristics depend on the nature of the binding forces. Soft agglomerates comprise particles held together by weak binding forces (i.e., van der Waals forces), and are broken apart during the formation of the green compacts. Normally, fine ceramic powders are formed by soft agglomerates because of the dominant role of the van der Waals forces. On the other hand, hard agglomerates comprise particles held together by strong binding forces (chemical bonds in solid bridges), and therefore are not broken during the formation [4,5] but remain even under the application of high compaction pressures. This is

\*Corresponding author. Tel.: +54 341 4495467, fax: +54 341 4495467x37.

E-mail address: [rcaruso@fceia.unr.edu.ar](mailto:rcaruso@fceia.unr.edu.ar) (R. Caruso).

highly undesirable because it induces packing inhomogeneities in the green body. Also, during sintering the agglomerates densify at temperatures insufficient for the elimination of the triple joints and porous zones, whose densification requires higher temperatures and/or longer sintering times [5]. Clearly, these problems can be avoided by using powders as fine as possible with soft agglomerates, as these characteristics enable good flowability, high packing density, and good resistance to green manipulations.

The quality of the sintered body also depends on the physicochemical characteristics of the powder. In this regards, the sol–gel method allows the synthesis of powders with well-controlled homogeneity, purity, reactivity, and particle morphology and size [6], although often these powders are formed by agglomerates of strongly bonded particles [7]. In the sol–gel process, precursors (usually metal alkoxides) undergo hydrolysis and condensation reactions, thus leading to an oxide network which is formed in the solution through inorganic polymerization reactions at room temperature [8]. These reactions play a significant role in modifying certain material properties [9]. At the beginning of the process, a few number of metal alkoxide molecules reacts by condensation, resulting in the formation of a bigger molecule, called cluster, that contains a few number of metallic centers. Then, the clusters grow by condensation reactions through two types of growth processes to form the gel. If the cluster reacts with other cluster the growth is called cluster–cluster; on the contrary, if the cluster reacts with a monomer the growth is called monomer–cluster [10].

It is known that the parameters of the sol–gel synthesis process affect notably the gel properties, and then the microstructure of the corresponding powders and their subsequent thermal evolution [9,11]. In turn, this affects the sintering behavior of the sol–gel powders. Therefore, understanding the mechanisms of sol–gel powder preparation is crucial to optimize the properties of Y-TZP ceramics. With these premises in mind, in the present work we have studied the effect of utilization of different parameters during the sol–gel synthesis, in particular solution pH and acetic acid addition, on the morphology, microstructure and thermal evolution of Y-TZP powders. The densification of the pellets obtained by pressing these powders was also analyzed.

## 2. Experimental

### 2.1. Powder preparation

Two starting solutions were prepared by stirring zirconium *n*-propoxide (ZNP; 70 wt% in *n*-propanol) and *n*-propanol (PrOH), in an anhydrous nitrogen atmosphere. After 1 h, distilled water was carefully added to the first solution (P<sub>1</sub>; 6:1 molar ratio). On the other hand, acetic acid and distilled water were added to the second solution (P<sub>2</sub>; 4:2:1 molar ratio). Other two solutions were also prepared by stirring ZNP, *n*-propanol, and HNO<sub>3</sub> as a catalytic agent in the anhydrous nitrogen atmosphere. After 1 h, distilled water was added to the third solution (P<sub>3</sub>; 6:1 molar ratio), and acetic acid and distilled water were added to the fourth solution (P<sub>4</sub>; 4:2:1 molar ratio). The Y<sub>2</sub>O<sub>3</sub>-doped solutions were obtained by adding yttrium

acetate (99.9% Aldrich) dissolved in propanol and nitric acid to the starting ZNP solution prior to the addition of acetic acid and water. The alcohol/ZNP molar ratio and yttria concentration were chosen to be 15 and 3 mol%, respectively. Powders were then obtained by gelification of the solutions and drying of the gels at 100 °C in air for 48 h. Pellets were prepared by uniaxial compaction (at 200 MPa) of the powders previously treated at 700 °C and crushed by a mortar and pestle for 5 min. Finally, the samples were sintered at 1200 °C for 2 h with a heating rate of 3 °C/min.

### 2.2. Characterization

The morphology of the as-obtained powders was studied by scanning electron microscopy (SEM) in a Philips SEM 515 and transmission electron microscopy (TEM) in a JEOL JEM-1010. Carbon content in the powders as a function of temperature from 100 to 1250 °C was determined in a LECO-200 induction furnace instrument. Specific surface areas and pore volume were obtained based on the Brunauer–Emmett–Teller (BET) method using a 2000 E Accosorb Micromeritics equipment; measurements were performed on as-prepared samples. X-ray diffraction (XRD) patterns were obtained at room temperature for the gels after heat-treatments in air at 700 and 1250 °C, the heating rate being 3 °C/min. After holding the powder for 2 h at the specified temperature, it was cooled by air quenching. XRD data were obtained over the 2θ=20–90° range (steps of 0.02°) and at 5 s per step. A Philips PW1700 diffractometer of 0.0018° instrumental broadening, with graphite monochromator and Cu Kα radiation was used. The diffractograms were analyzed by the Rietveld method, using the BGMN code. The pellet porosity was measured by the Archimedes method.

## 3. Results and discussion

It is known that the sol–gel method involves hydrolysis and condensation reactions starting from metallic precursors that lead to the gel formation. In the present case, during the hydrolysis reaction an alkoxide group is hydrolyzed to form a ZrOH group and alcohol, as follows:  $Zr(OPr)_4 + nH_2O \rightarrow Zr(OH)_n(OPr)_{4-n} + nPrOH$ . During condensation, two species with a metallic center (monomer) react originating a species with two metallic centers (dimer). Then, the condensation of these species continues to form bigger polymers. If the condensation involves two hydrolyzed species ( $Zr(OH)_n(OPr)_{4-n}$ ), then the reaction is named as oxolation, and is as follows:  $Zr(OH)_n(OPr)_{4-n} + Zr(OH)_n(OPr)_{4-n} \rightarrow (OH)_{n-1}(OPr)_{4-n}ZrOZr(OH)_{n-1}(OPr)_{4-n} + H_2O$ . On the other hand, if the reaction involves a hydrolyzed species and an alkoxide group ( $Zr(OPr)_4$ ), then it is named as alcoxolation, and is as follows:  $Zr(OH)_n(OPr)_{4-n} + Zr(OPr)_4 \rightarrow (OH)_{n-1}(OPr)_{4-n}ZrOZr(OPr)_3 + PrOH$ . While the reaction continues several metallic centers are joined together forming clusters. The gel formation could thus be visualized as the formation of a giant cluster.

With respect to the experimental results, the first differences between the samples were shown during the preparation process of those before the addition, depending on the case,

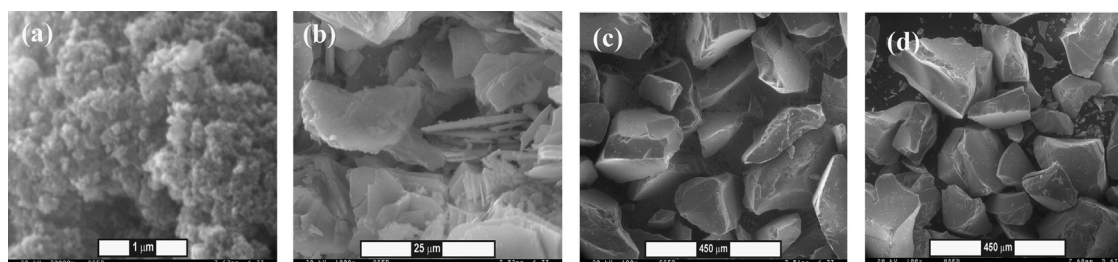


Fig. 1. SEM micrographs of the as-obtained powders: (a) P<sub>1</sub>, (b) P<sub>2</sub>, (c) P<sub>3</sub> and (d) P<sub>4</sub>.

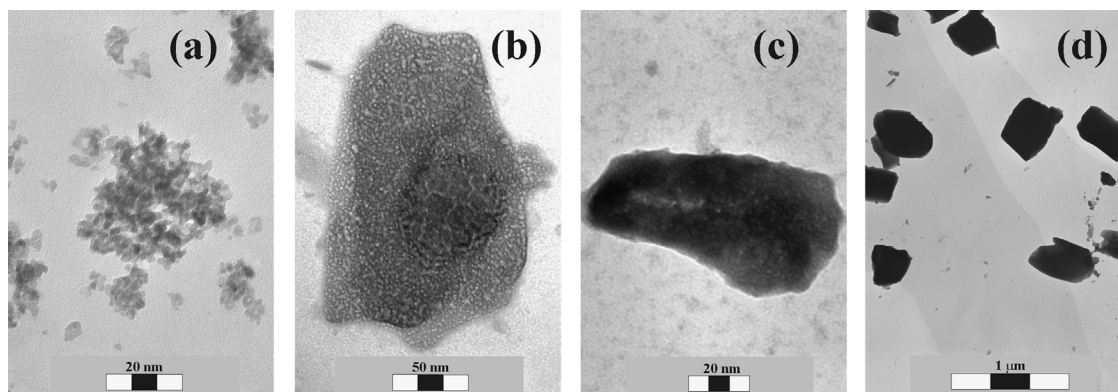


Fig. 2. TEM micrographs of the powders after breaking the agglomerates with a mortar and pestle: (a) P<sub>1</sub>, (b) P<sub>2</sub>, (c) P<sub>3</sub> and (d) P<sub>4</sub>.

of water and acetic acid. While the P<sub>2</sub> solution presented a heterogeneous aspect formed by a mixture of two phases, the rest of the solutions presented a homogeneous appearance.

The SEM micrographs in Fig. 1 show clear evidences of the existence of substantial differences among the powders prepared in this study. Thus, while the powder P<sub>1</sub> (Fig. 1a) exhibits the morphology of a porous material comprising small particles with smooth surfaces, the other three powders (Fig. 1b–d) comprise larger particles with a mean size of tens of microns (powder P<sub>2</sub>, Fig. 1b) or hundreds of microns (powders P<sub>3</sub> and P<sub>4</sub>, Fig. 1c and d, respectively) as well as faceted surfaces. Furthermore, the particles in the powders P<sub>1</sub> and P<sub>2</sub> were found to be actually soft agglomerates which could be disintegrated simply by manual contact. In contrast, powders P<sub>3</sub> and P<sub>4</sub> were made of very hard particles with strong agglomeration, which in addition were quite difficult to be broken by the mortar and pestle. Nevertheless Fig. 2 shows representative TEM micrographs of all powders after being broken with the mortar and pestle. It can be seen that the powder P<sub>1</sub> comprise particles with an average size of 10 nm (Fig. 2a), whereas the corresponding particle sizes for the powders P<sub>2</sub> and P<sub>3</sub> range between 400 and 500 nm (Fig. 2b and c) and for the powder P<sub>4</sub> are much larger in the order of 1 μm (Fig. 2d).

Shown in Fig. 3 are the results of the carbon elementary analysis (in wt%) obtained for the powders heat-treated at different temperatures for 1 h in air. It can be seen that the powder P<sub>2</sub>, which was prepared at pH 5 under the presence of acetic acid in the medium, exhibits the greatest amount of organic residuals at 100 °C. Also, it can be observed that all powders, except P<sub>1</sub>, requires of thermal treatments above

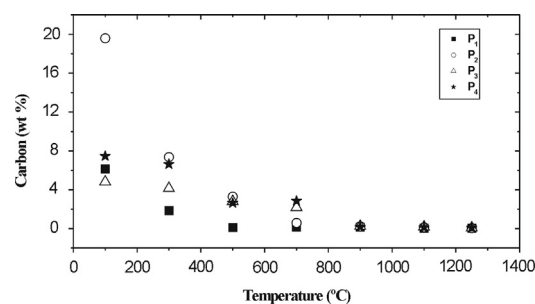


Fig. 3. Residual carbon content in the powders as a function of annealing temperature in air.

700 °C to totally eliminate the organic products of the sol–gel synthesis.

It is clear that the different conditions of sol–gel processing have influenced the characteristics of the YSZ powders. Thus, the solutions P<sub>1</sub> and P<sub>3</sub> were prepared using a quantity of water greater than the stoichiometric one, which enables the hydrolysis of all propoxide groups of the metallic precursor. On the other hand, although the hydrolysis rate of alkoxides of transition metals is high, the nitric acid presence in the sol–gel solutions provides a high concentration of hydrogen ions H<sup>+</sup> that reduces the nucleophilic character of water and consequently the hydrolysis rate [12]. For this reason, the precursor solution P<sub>1</sub> (without HNO<sub>3</sub>) undergoes a faster hydrolysis than the solutions P<sub>3</sub> and P<sub>4</sub>, which results in the formation of zirconium preferentially linked to OH-groups instead of propoxide groups thus favoring the fact that condensation occurs through the oxolation mechanism. On the contrary, the hydrolysis rate in the precursor solution P<sub>3</sub> is

slower due to the high concentration of hydrogen ions  $H^+$ , and therefore the condensation reaction takes place in the presence of less hydrolyzed species, thus promoting that the condensation which occurs through the alcoxolation mechanism.

The TEM observations in Fig. 2 also reveal very interesting results. Thus, the morphology of the particles of the powder  $P_1$  could be understood by associating the generation of each particle with the growth of an initial cluster whose size increases according to the mechanism of monomer–cluster growth. In this way, the growth of this initial cluster is restricted when no more monomers are available in the solution, thus limiting the size of the final particles and conditioning their small size. These small particles are held together by weak binding forces, and therefore the agglomerates are soft. In contrast, the morphology of the particles in the powders  $P_3$  and  $P_4$  could be attributed to the growth of the initial clusters which occurred by the cluster–cluster mechanism. With this mechanism, the joining of the clusters led to the formation of an entire network of zirconium atoms, oxygen, and organic groups. Hence, by the means of elimination of the solvent at 100 °C, the wet gel undergoes a volume contraction resulting in a dried gel structure that is more rigid, and the stresses cause its fracture. The particles of the powders  $P_3$  and  $P_4$  would acquire their angular shape by strong binding forces. The similarity between the particles in the powders  $P_3$  and  $P_4$  indicate that the presence of nitric acid in the precursor solutions of these powders is a dominant factor in determining their morphology.

Table 1 lists the specific surface area of the powders calcined at 100 °C. It can be seen that the powders resulting from the solutions without acetic acid (i.e.,  $P_1$  and  $P_3$ ) present very high values of specific surface area, which is higher than the values for the powders prepared in the presence of acetic acid in the medium (i.e.,  $P_2$  and  $P_4$ ). Also, it can be deduced that the specific surface area of the powders does not seem to be significantly influenced by their average particle size. Table 2 lists the micropore and mesopore volumes of the powders calcined at 100 °C. It can be seen that the powder  $P_1$  has the greatest mesopore volume. Also, the powder  $P_3$  has a very low mesopore volume (0.028 cm<sup>3</sup>/g) with respect to the powder  $P_1$  (0.402 cm<sup>3</sup>/g). This would indicate that the mesopore presence in the powders is not the main source of the high values of specific surface area measured for these

Table 1  
Specific area (m<sup>2</sup>/g) of the powders dried at 100 °C.

$P_1$	$P_2$	$P_3$	$P_4$
389.0	5.8	230.5	0.4

Table 2  
Micropore and mesopore volumes (cm<sup>3</sup>/g) for the powders dried at 100 °C.

Volume (cc/g)	$P_1$	$P_2$	$P_3$	$P_4$
Micropores	0.145	0.004	0.109	0.001
Mesopores	0.402	0.021	0.028	0.002

powders. On the other hand, the micropore volume of the powders  $P_1$  and  $P_3$  is greater than that of the other two powders. Also, the micropore volumes do follow the trends of the specific surface area data, and therefore the micropore volumes are mainly responsible for the specific surface area of the powders. Consequently, future works should be focused on studying the causes of micropore formation. In principle it is reasonable to think that this should be related to the residue elimination of the sol–gel synthesis during the drying of the powders at 100 °C, as well as to the network characteristics formed during the synthesis.

Fig. 4 shows the XRD patterns of the powders calcined at 700 °C. It can be seen that the powder  $P_2$  comprises a combination of tetragonal and monoclinic  $ZrO_2$  phases, whereas the other powders comprise only tetragonal  $ZrO_2$  phase. Moreover, as shown in Fig. 5, after the heat treatment at

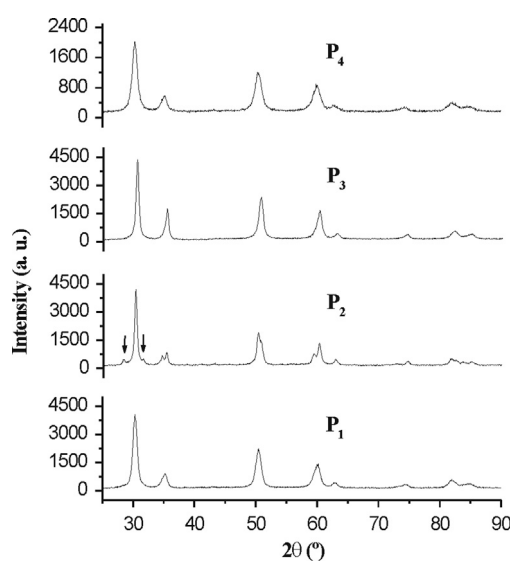


Fig. 4. Experimental XRD patterns of the powders after annealing for 2 h at 700 °C.

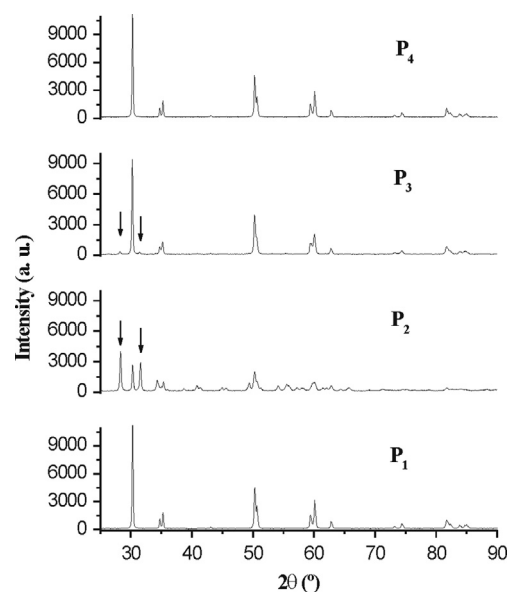


Fig. 5. Experimental XRD patterns of the powders after annealing for 2 h at 1250 °C.

Table 3  
Percentage of tetragonal phase.

Temperature (°C)	P <sub>1</sub>	P <sub>2</sub>	P <sub>3</sub>	P <sub>4</sub>
700	98	89	100	100
1250	100	23	91	100

Table 4  
Pellet porosity after sintering at 1200 °C for 2 h in air.

P <sub>1</sub>	P <sub>2</sub>	P <sub>3</sub>	P <sub>4</sub>
0.20	0.42	0.42	0.38

1250 °C (Fig. 5) the powders P<sub>1</sub> and P<sub>4</sub> are still formed entirely by tetragonal ZrO<sub>2</sub>, the powder P<sub>3</sub> contains traces of monoclinic ZrO<sub>2</sub>, and the powder P<sub>2</sub> is mostly monoclinic ZrO<sub>2</sub>. Table 3 lists the percentages of tetragonal phase retained in each powder, calculated using the Rietveld method. It is important to explain the reasons for the complete retention of tetragonal ZrO<sub>2</sub> in the powders P<sub>1</sub> and P<sub>4</sub>. It has been proposed that this can be due to different causes [12,13], one of which is the crystallite size [14]. The crystallite sizes calculated for the powders annealed at 1250 °C were quite similar, that is, 163, 96, 131, and 156 nm for P<sub>1</sub>, P<sub>2</sub>, P<sub>3</sub> and P<sub>4</sub>, respectively. Therefore, the crystallite size does not seem to be responsible for the complete retention of tetragonal ZrO<sub>2</sub> in the powders P<sub>1</sub> and P<sub>4</sub>. It is proposed that the cause of the stability of the tetragonal phase in these powders is directly related to the sol–gel synthesis. In particular, during the heat treatment the Y<sub>2</sub>O<sub>3</sub> doping can either diffuse into the ZrO<sub>2</sub> crystal lattice or segregate at grain boundaries, depending on how the yttrium atoms were combined with the zirconium atoms in the gel network during the synthesis process. In this context, the presence of monoclinic phase could be attributed to an inhomogeneous distribution of yttrium and zirconium ions in the sol–gel solutions, due to the conditions used in each synthesis process, so that stabilization of the tetragonal phase is not possible [15]. This hypothesis, of course, needs further confirmation in future works.

Finally, Table 4 lists the porosity of the compacts sintered at 1200 °C at 3 °C/min for 2 h in air. While the compact P<sub>1</sub> has a porosity of 20%, the others have porosities around 40%. The powder P<sub>1</sub> thus exhibits better densification behavior than the rest of the powders, which could be due to various factors such as the size and reactivity of the particles, the specific surface area, and the degree of green-body densification. The greatest specific surface area and the presence of soft agglomerates in the as-prepared powder P<sub>1</sub> benefit its densification during the subsequent sintering. On the other hand, the easy elimination of organic residuals from the powder P<sub>1</sub> (see Fig. 3) also hinders the formation of hard agglomerates and loss of specific surface area.

#### 4. Concluding remarks

1. The conditions of sol–gel synthesis influence the hydrolysis and condensation process of zirconium *n*-propoxide, and therefore the features of the obtained powder. The solution pH impacts significantly the hydrolysis of zirconium *n*-propoxide. The presence of nitric acid in the sol–gel solutions provides a high concentration of H<sup>+</sup> ions that reduces the nucleophilic character of water and consequently the hydrolysis rate. Under these conditions, as happens in the case of the precursor solutions P<sub>3</sub> and P<sub>4</sub>, the hydrolysis rate is slower and the condensation takes place by the alcoxolation mechanism. On the contrary, under lower concentration of H<sup>+</sup> ions, as happens in the solution P<sub>1</sub>, a faster hydrolysis takes place and the condensation occurs by the oxolation mechanism.
2. The synthesis process has a notable effect on the morphology of the resulting ZrO<sub>2</sub> powders. The precursor gel P<sub>1</sub> was developed by the monomer–cluster growth process, and for this reason this powder comprises small particles (10 nm) and soft agglomerates. On the other hand, the precursor gels P<sub>3</sub> and P<sub>4</sub> were developed by the cluster–cluster growth process, and thus these powders are formed by larger particles (mean size between 500 and 1000 nm) and hard agglomerates.
3. Powders of metastable tetragonal ZrO<sub>2</sub> have been successfully prepared using the sol–gel method. Stabilization achieved with the present yttria concentration is maintained during sintering up to at least 1200 °C. Tetragonal ZrO<sub>2</sub> powders are obtained only if a homogeneous distribution of yttrium and zirconium cations in the sol–gel solution is achieved.
4. The micropore volume is the main cause that confers high specific surface area to the ZrO<sub>2</sub> powders prepared by the sol–gel method. The specific surface area is not significantly influenced by the particle size or by the mesopore volume.
5. The smaller particle size and the presence of soft agglomerates in the as-prepared ZrO<sub>2</sub> powders, achieved by the judicious control of the sol–gel synthesis conditions, benefit their densification during sintering.

#### Acknowledgments

This work was partly supported by Conicet (Argentina), the “Agencia Nacional de Promoción Científica y Tecnológica” (National Agency for Scientific and Technologic Promotion) of Argentina and the Universidad de Extremadura (España).

#### References

- [1] M. Ruhle, N. Claussen, H. Heuer, *Advances in Ceramics*, in: N. Claussen, M. Ruhl, H. Heuer (Eds.), The American Ceramic Society, Westerville, OH, 1984 (p. 352).
- [2] K. Tsukuma, et al., *J. Am. Ceram. Soc.* 68 (2) (1985) C-56.
- [3] M.H. Bocanegra-Bernal, Agglomeration of magnesia powders precipitated from sea water and its effects on uniaxial compaction, *Mater. Sci. Eng. A* 333 (2002) 176–186.

- [4] M. Taha, J. Palaetto, Y. Jorand., G. Fantozzi, A. Samdi, M. Jebrouni, B. Duran., Compactation and sintering behavior of zirconia powders, *J. Eur. Ceram. Soc.* 15 (1995) 759–768.
- [5] F.F. Lange, Sinterability of agglomerated powders, *J. Am. Ceram. Soc.* 67 (2) (1984) 83–89.
- [6] L.L. Hench, D.R. Ulrich, *Ultrastructure Processing of Ceramics, Glasses and Composites*, J. Wiley, New York, 1984.
- [7] V. Srdić, M. Winterer, Comparison of nanosized zirconia synthesized by gas and liquid phase methods, *J. Eur. Ceram. Soc.* 26 (2006) 3145–3151.
- [8] J. Livage, F. Beteille, C. Roux, M. Chatry, P. Davidson, *Acta Mater.* 46 (1998) 743.
- [9] B.E. Yoldas, *J. Mater. Sci.* 21 (1986) 1080.
- [10] C.J. Brinker, G.W. Scherer, *Sol–Gel Science: the Physics and Chemistry of Sol–Gel Processing*, Academic Press, San Diego, 1990.
- [11] R. Caruso, et al., *J. Sol–Gel Sci. Technol.* 3 (1994) 241.
- [12] M.C. Caracoche, P. Rivas, M. Cervera, R. Caruso, E. Benavidez, O. de Sanctis, S.R. Mintzer, Nanostructural study of sol–gel-derived zirconium oxides, *J. Mater. Res.* 18 (1) (2003) 208–215.
- [13] A.V. Chadwick, G. Mountjoy, V.M. Nield, I.J.F. Poplett, M.E. Smith, J.H. Strange, M.G. Tucker, Solid-state NMR and X-ray studies of the structural evolution of nanocrystalline zirconia, *Chem. Mater.* 13 (2001) 1219–1229.
- [14] R.C. Garvie, *J. Phys. Chem.* 82 (1978) 218.
- [15] C. Kuo, Y. Lee., K. Fung, M. Wang, Effect of  $Y_2O_3$  addition on the phase transition and growth of YSZ nanocrystallites prepared by a sol–gel process, *J. Non-Cryst. Solids* 351 (2005) 304–311.